Pflugers Arch – Eur J Physiol (2005) 450: 415–428
DOI 10.1007/s00424-005-1399-1

ION CHANNELS, TRANSPORTERS

**Lars M. Holm · Thomas P. Jahn · Anders L. B. Møller
Jan K. Schjoerring · Domenico Ferri · Dan A. Klaerke
Thomas Zeuthen**

NH_3 and NH_4^+ permeability in aquaporin-expressing *Xenopus* oocytes

Received: 21 December 2004 / Accepted: 17 February 2005 / Published online: 30 June 2005

Abstract We have shown recently, in a yeast expression system, that some aquaporins are permeable to ammonia. In the present study, we expressed the mammalian aquaporins AQP8, AQP9, AQP3, AQP1 and a plant aquaporin TIP2;1 in *Xenopus* oocytes to study the transport of ammonia (NH_3) and ammonium (NH_4^+) under open-circuit and voltage-clamped conditions. TIP2;1 was tested as the wild-type and in a mutated version (tip2;1) in which the water permeability is intact. When AQP8-, AQP9-, AQP3- and TIP2;1-expressing oocytes were placed in a well-stirred bathing medium of low buffer capacity, NH_3 permeability was evident from the acidification of the bathing medium; the effects observed with AQP1 and tip2;1 did not exceed that of native oocytes. AQP8, AQP9, AQP3, and TIP2;1 were permeable to larger amides, while AQP1 was not. Under voltage-clamp conditions, given sufficient NH_3, AQP8, AQP9, AQP3, and TIP2;1 supported inwards currents carried by NH_4^+. This conductivity increased as a sigmoid function of external [NH_3]: for AQP8 at a bath pH (pH_e) of 6.5, the conductance was abolished, at pH_e 7.4 it was half maximal and at pH_e 7.8 it saturated. NH_4^+ influx was associated with oocyte swelling. In comparison, native oocytes as well as AQP1 and tip2;1-expressing oocytes showed small currents that were associated with small and even negative volume changes. We conclude that AQP8, AQP9, AQP3, and TIP2;1, apart from being water channels, also support significant fluxes of NH_3. These aquaporins could support NH_4^+ transport and have physiological implications for liver and kidney function.

Keywords Ammonia · Ammonium · Aquaporins · Conduction · Oocytes · Mitochondria · Liver · Kidney · Plant

L. M. Holm · D. A. Klaerke · T. Zeuthen (✉)
Nordic Centre for Water Imbalance Related Disorders.
Department of Medical Physiology, Panum Institute,
University of Copenhagen, 2200N, Denmark
E-mail: tzeuthen@mfi.ku.dk

T. P. Jahn · A. L. B. Møller · J. K. Schjoerring
Plant Nutrition Laboratory, Department of Agricultural Sciences,
Royal Veterinary and Agricultural University, 1871F-C, Denmark

D. Ferri
Department of Zoology, Laboratory of Histology
and Comparative Anatomy, University of Bari, Italy

Introduction

Aquaporins (AQP) are membrane proteins that conduct water passively. To date, thirteen types of aquaporins have been found in mammals, AQP0–AQP12, located in both plasma membranes and organelles. Some aquaporins are specific for water while others are also permeable to small hydrophilic molecules such as urea and glycerol [2]. We have recently shown by heterologous expression in both yeast and *Xenopus* oocytes that human AQP8 and a plant aquaporin TaTIP2;1 (TIP2;1) are also permeable to ammonia. In a mutant yeast that is deficient in ammonia transport, AQP8 and TIP2;1 restores the ability for cell growth when NH_4^+ is present in the external medium. In *Xenopus* oocytes, AQP8 and TIP2;1 transport NH_3, as well as the analogues formamide and methylammonia. As a control, we constructed a mutant of the plant aquaporin Tatip2;1-I^{184} H, G^{193} C (tip2;1), which was unable to restore ammonia transport to the deficient yeast. AQP1 served as a control in both yeast and oocytes since this aquaporin does not support ammonia transport in either system [21].

In the present investigation, we extended these investigations and included other aquaporins, primarily those found in nitrogen-handling organs such as the liver and the kidney. Most experiments were performed on rat AQP8, which, among a wide range of organs, has been detected in the testis, liver and kidney and in the small and large intestine [7, 10, 12, 14, 19, 25, 28, 36]. In most cell types, AQP8 is located intracellularly but can also be sorted to plasma membranes. In mouse

hepatocytes, for instance, it has been detected in mitochondria, smooth endoplasmic reticulum, sub-apical vesicles and canalicular (apical) membranes [12]. We also examined AQP9, which is expressed in liver, particularly in the sinusoidal plasma membranes of the hepatocytes [8, 19, 20, 36, 40, 41] and AQP3 from the basolateral membranes of kidney collecting tubules (for reviews see [35, 38]). As controls, we used AQP1, which is permeable only to water [30], and the mutant tip2;1 in which ammonia transport was abolished but, as we show here, water transport retained.

Xenopus oocytes depolarize in the presence of NH_4Cl, [5, 9, 33, 39]. Surprisingly, we found that such depolarizations were much more pronounced in oocytes expressing the ammonia-permeable aquaporins. This functional NH_4^+ permeability was studied for AQP8-, AQP9-, AQP3- and TIP2;1-expressing oocytes under open-circuit and voltage-clamp conditions. The nature and direction of the ionic flux were determined from ion substitutions and by continuous measurements of oocyte volume. We discuss two possibilities: (1) NH_3 permeates the aquaporins and stimulates endogenous pH-sensitive permeabilities of the oocyte or (2) the presence of NH_3 enables NH_4^+ to permeate the aquaporin itself. In aqueous solutions of NH_4Cl, ammonium (NH_4^+) is present together with its conjugate base ammonia (NH_3), see Appendix. In the following, the term "ammonia" will be used when referring to both NH_3 and NH_4^+ in general, while the chemical symbols will be used to refer to NH_4^+ and NH_3 specifically.

Materials and methods

Preparation of mRNA, injection into and maintenance of the *Xenopus* oocytes, tracer, voltage-clamp and oocyte volume experiments were carried out as described previously [18, 29, 47, 48]. All oocyte collection procedures conformed to Danish Animal Ethics Regulations. cRNA was synthesized by the mCAP in vitro transcription kit from Stratagene and T3 or T7 RNA polymerase was used for run-off transcription of sense-cRNA. Stage V–VI oocytes were isolated and defolliculated with collagenase (Boehringer, Mannheim, Germany or Sigma-Aldrich, Copenhagen, Denmark). Human AQP1 was obtained from American Type Culture Collection (ATCC 99538), while rat AQP3 and AQP9 plasmids were gifts from S Nielsen. The rat AQP8 plasmid, pXβG-rAQP8, was constructed by G. Calamita by inserting the rat AQP8 open reading frame into the *Bam*HI site of the pXβG-ev1 vector [37]. Immunofluorescence studies showed oolemma expression of AQP8 (D. Ferri, G. Calamita, personal communication). Ta-tip2;1 was employed as the wild-type (TIP2;1) or as the double mutant (tip2;1) in which ile184 is changed to his and gly193 to cys [21]. Each oocyte was injected with 50 ng cRNA and incubated at 19°C in Kulori medium (mM): 90 NaCl, 1 KCl, 1 $CaCl_2$, 1 $MgCl_2$, 5 HEPES, pH 7,4, 192 mosm/l. To reduce variability in transport parameters, oocytes were allowed to recover from surgery, enzymatic treatment and injection for 4–8 days before experiments [1]. Only oocytes with membrane potentials more negative than −20 mV were used.

For NH_3 uptake measurements, 20 oocytes were washed twice in unbuffered solution (mM): 90 NaCl, 20 mannitol, 2 KCl, 1 $CaCl_2$, 1 $MgCl_2$, 214 mosm/l and placed in a stainless-steel net, 8 mm in diameter and 2 mm deep, 0.5 mm mesh. The net was bathed in a well-stirred test solution of low buffer capacity and the change in bath pH recorded. The solution contained (mM): 70 NaCl, 20 mannitol, 20 NH_4Cl, 2 KCl, 1 $CaCl_2$, 1 $MgCl_2$, 0.1 HEPES, 214 mosm/l. The solution was titrated with 1 M NaOH to pH 6.5, 7.4 or 8.5. The resulting buffer capacity of the pH 6.5 solution was 0.125, of the 7.4 solution 0.625, and of the pH 8.5 solution 5.0 mM/pH. The buffer capacity was found by titrating the test solution with 1 M HCl. The test solution (2.2 ml) was held in a concentric beaker, 16 mm in diameter and 16 mm high. The net containing the 20 oocytes was placed about 3 mm above the bottom, giving room for a small magnetic stirrer, 270 rpm. The pH changes were measured by a small pH-electrode (XC 161 microelectrode, Radiometer, Denmark) inserted through a tight-sealing lid of Teflon. If any oocytes ruptured during the experiment, the result was discarded.

The permeabilities for formamide (NH_2CONH_2), P_{form}, and for methylammonia/methylammonium (MeA, $NH_2CH_3/NH_2CH_4^+$), P_{MeA}, were derived from the uptake of [^{14}C]formamide and [^{14}C]methylamine-HCl. Five oocytes were transferred in to a stainless-steel net to a test solution containing 4.0 μCi/ml [^{14}C]formamide or [^{14}C]methylamine-HCl and 20 mM unlabelled formamide or methylamine-HCl. The resulting tracer concentration of formamide was 78 μM and 69 μM for methylamine-HCl. The test solutions were stirred on a vibration table (3 rotations/s, amplitude 6 mm) during uptake. To terminate uptake, oocytes, while still in the net, were rinsed in a stream of ice-cold Kulori medium for about 30 s. Subsequently, each oocyte was transferred to a scintillation vial and vortexed in 200 μl 20% sodiumdodecylsulphate. After addition of 2 ml scintillation fluid (Packard Opti-Fluor), oocytes were transferred to a scintillation counter (Packard Tri-Carb). The uptakes are presented relative to the concentration in the bathing solution (i.e. in units of cm). Accordingly, the uptake rate (uptake divided by the time of uptake) has units of permeability (cm/s).

Membrane potentials, clamp currents and oocyte volumes were measured simultaneously as previously described [29, 48]. Briefly, oocytes were placed in a continuously perfused 30-μl chamber, in which the bathing solution could be changed within 5 s (90% complete). The oocytes were impaled with two microelectrodes that served to determine the membrane potential and to stabilize the oocytes. The presence of microelectrodes did not affect the volume measurements. Oocyte volume was monitored on-line from below via an

inverted microscope with an accuracy of 0.03%. The oocytes were illuminated from above via a Plexiglas rod, the end of which also served as a lid to the chamber. The temperature of the experimental chamber was 23°C. The control bathing solution contained (mM): 90 NaCl, 20 mannitol, 2 KCl, 1 $CaCl_2$, 1 $MgCl_2$, 10 HEPES or TRIS, 214 mosm/l, pH 7.4. Various [NH_4Cl] were obtained by isosmotic replacement of NaCl. Osmolarity was checked in duplicate for each solution by freezing point depression (Roebling), and appropriate amounts of mannitol were added to obtain isosmolarity to within 1 mosm/l.

The osmotic water permeability (L_p) is obtained from:

$$J_v = (-dV/Vdt)V_o = L_p A \Delta\pi, \quad (1)$$

where J_v is the volume flow into the oocyte, $-d\,V/V d\,t$ the initial relative rate of volume change (usually measured within 10 s), V_o the initial oocyte volume and A the true oocyte surface area. With an average diameter of 1.35 mm, oocytes have an apparent spherical surface area of 5.9 mm^2. Folding of the membrane increases this area by a factor of 9 [44] to give a true surface area A of 0.53 cm^2. R is the gas constant and T the absolute temperature. $\Delta\,\pi$ is the transmembrane concentration difference of impermeable solutes such as mannitol or sucrose, usually 20 mosm/l. In this paper, L_p is given in units of 10^{-5} cm s^{-1} (osm $l^{-1})^{-1}$This unit can be transformed into cm/s by multiplying with the molar concentration of water, 55 M.

The coupling between a permeable osmolyte (s) and a volume flux can be characterized by a reflection coefficient σ_s, which is a measure of the ability of the osmolyte to produce volume changes:

$$L_{p,s} = \sigma_s L_p, \quad (2)$$

where $L_{p,s}$ is the apparent water permeability obtained with s as osmolyte and L_p the true osmotic water permeability obtained with an impermeable osmolyte, in the present study sucrose or mannitol. In conventional irreversible thermodynamics [22], σ_s has the form

$$\sigma_s = 1 - RTP_s(\Delta x/\varphi_w)f_{sw}, \quad (3)$$

where $\Delta x/\phi_w$ is a constant defined by the ratio of the membrane thickness to the volume fraction of water and f_{sw} a frictional factor coupling the solute and water in the pore. It follows that $\sigma_s > 1$ is evidence for significant, non-zero values of P_s and f_{sw}.

Intracellular pH (pH_i) was measured by means of double-barrelled, H^+-selective microelectrodes similar to those previously described [45, 46]. We used theta glass with a thick septum (TST150-6; WPI, Sarasota, Fla., USA). The reference barrel was filled with 1 M KCl and had a resistance of up to 10 MΩ. We used the hydrogen ionophore II, cocktail A (95297) from Fluka.

All data are given as means ± SE; n (in brackets) is the number of oocytes unless otherwise stated. $P < 0.05$ (Student's t-test) was taken as the level of significance. All experiments were performed at room temperature 22–24°C

Results

In the first part, we show that NH_3 and electroneutral analogues are transported across oocyte membranes that express AQP8, AQP9, AQP3, or the wild-type TIP2;1; we also show that AQP1 and the mutated tip2;1 do not share these properties. In the second part, we show that expression of NH_3-permeable aquaporins increases the

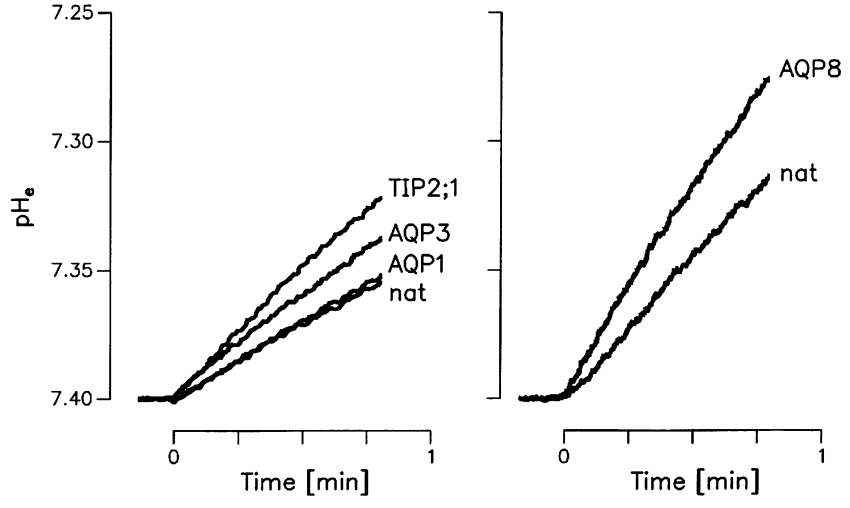

Fig. 1 Uptake of NH_3 into aquaporin (AQP or TIP)-expressing oocytes. Oocytes (20 cells) were added abruptly to 2.2 ml well-stirred solution containing 20 mM NH_4Cl at an extracellular pH (pH_e) of 7.4 and with a low buffer capacity (see Materials and methods). The initial rate of acidification of the bathing solution is a measure of the rate of uptake of NH_3 relative to that of NH_4^+ (see Appendix). *Left*: uptake into oocytes expressing TIP2;1, AQP3 and AQP1 and into native (*nat*) oocytes from the same batch. *Right*: uptake into AQP8-expressing oocytes and into native oocytes from the same batch. The acidification induced by the expression of the aquaporins above that of the corresponding native oocytes is given in Table 1

Table 1 Initial rates of acidification (units: 10^{-11} mol H^+/s per oocyte) of the bathing solution induced by the addition of oocytes expressing various aquaporins (*AQP*, *TIP*, Fig. 1), corrected for that of native oocytes from the same batch; experiments as in Fig. 1. Rates are calculated as the product of the initial rate of change in bath pH (pH_e) and the buffer capacity of the bathing solution a and are given per oocyte. The solutions contained 70 mM Na^+ and 20 mM NH_4^+ and had low buffer capacities (see Materials and methods). At pH_e 7.4 or 8.5, the corresponding $[NH_3]$ were 0.28 or 3.6 mM respectively. *NS*: non-significant difference between the rate of acidification of AQP-expressing and native oocytes from the same batch. In experiments at pH_e 6.5, there were no significant effects for the mammalian aquaporins (not shown). *Numbers* in *parentheses* are number of experiments using 20 oocytes each. The osmotic water permeabilities (L_p) for each group of oocytes are given in the *bottom* row in which the *numbers* in *parentheses* are the numbers of single oocytes

pH_e	AQP8	AQP9	AQP3	AQP1	TIP2;1	tip2;1
7.4	4.4 ± 2.0 (6) ($P < 0.03$)	3.6 ± 1.0 (7) ($P < 0.005$)	2.3 ± 0.7 (11) ($P < 0.005$)	1.0 ± 0.8 (3) NS	6.0 ± 0.9 (6) ($P < 0.0007$)	0.012 ± 0.12 (6) NS
8.5	46.0 ± 15.2 (4) ($P < 0.03$)	28.4 ± 6.0 (7) ($P < 0.0005$)	18.8 ± 6.0 (7) ($P < 0.02$)	12.8 ± 7.2 (5) NS		
L_p [$\times 10^{-5}$ cm s^{-1} (osm $l^{-1})^{-1}$]	5.7 ± 0.43 (9)	1.5 ± 0.17 (8)	4.1 ± 0.4 (14)	5.3 ± 0.5 (10)	4.7 ± 0.6 (4)	4.8 ± 0.7 (4)

NH_4^+ conductivity of *Xenopus* oocyte membranes significantly.

Transport of NH_3

If NH_3 is transported into a cell faster than its conjugate acid NH_4^+, the extracellular solution will acidify; see Appendix. Accordingly, when oocytes (20 cells) were added abruptly to a well-stirred bathing solution containing NH_4Cl and with a low buffer capacity, progressive acidification of extracellular pH (pH_e) was observed (Fig.1). The bathing solution contained 20 mM NH_4^+ (replacing Na^+) and pH_e was adjusted to 8.5, 7.4, or 6.5, equivalent to $[NH_3]$ of 3.6, 0.28 or 0.036 mM respectively. At pH_e 7.4 and 8.5, the rates of acidification observed with AQP8, AQP9, AQP3, and TIP2;1 were higher than those observed with native oocytes from the same batch (Fig. 1, Table 1). It appears that expression of either AQP8, AQP9, AQP3, or TIP2;1 induced an influx of NH_3 that exceeded that of the corresponding native oocytes. Oocytes expressing AQP1 or tip2;1 did not differ from native oocytes. Taken together with the data from the expression studies using yeast mutants deficient in ammonium transport [21], this suggests that these aquaporins do not support any significant transport of either NH_3 or NH_4^+. The inability to transport NH_3 is not due to a particularly low expression level of these aquaporins as estimated from the uniform L_p values of the oocytes (Table 1). At pH_e 6.5 we observed no significant influxes of NH_3, except for oocytes expressing TIP2;1 for which the initial rate of acidification was $0.96 \pm 0.20 \times 10^{-11}$ mol H^+/s ($n = 7$) above that of AQP 1.

The AQP-induced uptakes were related roughly linearly with the $[NH_3]$ and correspond to a P_{NH3} of about 2×10^{-4} cm/s for AQP8, AQP9, and TIP2;1, assuming an oocyte surface area of 0.6 cm^2 (see Materials and methods); P_{NH3} for AQP3 was about half this. The uptake of NH_3 into native oocytes varied with the season and probably reflects differences in lipid composition. For experiments performed in spring, it was 1.6 ± 0.12 ($n = 6$) at pH_e 6.5, 8.4 ± 0.4 ($n = 20$) at pH_e 7.4, and 50.4 ± 3.2 ($n = 5$) at pH_e 8.5 (in units of 10^{-11} mol H^+/s per oocyte), and about double this for experiments performed in late autumn. This variation does not affect our estimates of the AQP-induced uptake of NH_3; these were obtained as the difference between uptakes in AQP-expressing oocytes and native oocytes from the same batch. The native oocytes had an L_p of $0.35 \pm 0.06 \times 10^{-5}$ cm s^{-1} (osm $l^{-1})^{-1}$; this parameter showed no seasonal variation.

Transport of formamide and methylammonia/methylammonium (MeA)

The expression of AQP8, AQP9, AQP3, and TIP2;1 increased the uptake of [^{14}C]formamide above that of native oocytes. The uptake into AQP8-expressing oocytes was a linear function of time for the first 0.5 min (Fig. 2a); the corresponding line of regression had a slope of $29.8 \pm 1.3 \times 10^{-7}$ cm/s, ($n = 14$) and its intercept with the *y*-axis was $0.029 \pm 0.028 \times 10^{-4}$ cm, not significantly different from zero. Accordingly, this defines a permeability (P_{form}) of $29.8 \pm 1.3 \times 10^{-7}$ cm/s. Uptakes at later times were not linear and probably reflect unstirred layers and uptake into secondary compartments such as organelles. Uptake into the native oocytes from the same batch was linear and could be described by a permeability of $9.2 \pm 0.6 \times 10^{-7}$ cm/s, $n = 20$; Fig. 2a. The permeabilities for AQP9, AQP3, TIP2;1, and AQP1 were determined from uptakes obtained at 0.5 min and are given in Table 2. The uptake of formamide into AQP1-expressing oocytes was not different from that of native oocytes.

Similar data were obtained with [^{14}C]MeA. The uptake into AQP8-expressing oocytes was linear for the first 2 min (Fig. 2b); the corresponding line of regression had a slope of $5.3 \pm 0.3 \times 10^{-7}$ cm/s, ($n = 16$) and its intercept with the *y*-axis was $-0.029 \pm 0.023 \times 10^{-4}$ cm, not significantly different from zero. This defines a permeability (P_{MeA}) of $5.3 \pm 0.3 \times 10^{-7}$ cm/s (Table 2). For the corresponding native oocytes, uptake was linear for the first 2 min indicative of a P_{MeA} of $3.0 \pm 0.1 \times 10^{-7}$ cm/s (Fig. 2b). P_{MeA} for AQP9-, AQP3- and TIP2;1-expressing oocytes was also larger than that of native oocytes (Table 2). The uptake into

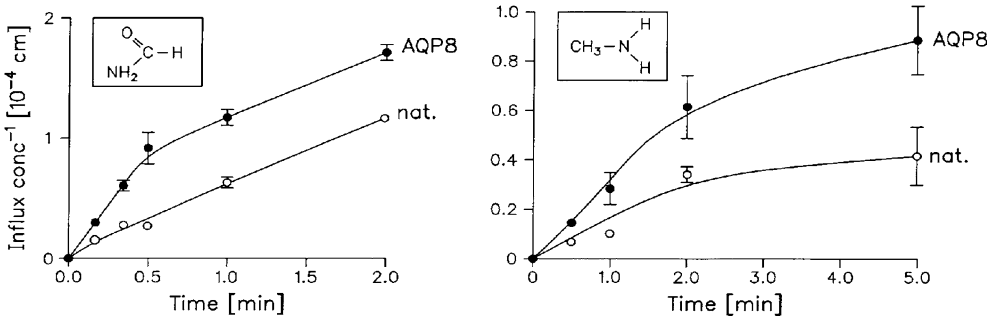

Fig. 2a,b Uptake of [^{14}C]formamide (**a**) and [^{14}C]methylammonia/methylammonium (**b**). AQP8-expressing and corresponding native oocytes were from the same batch. The *insets* show the chemical structures. Uptake has units of cm: moles taken up per surface area (cm^2) divided by the concentration in the test solution (mol/cm^3). In this way, the initial slopes of the lines, determined from regression analysis (see text), define the permeability P (cm/s) (see Table 2). Each *point* represents data from between three and six oocytes, the SE is shown if larger than the *symbol*

AQP3-expressing oocytes became significantly larger than that of native oocytes only after 2 min (data not shown). The uptake of MeA into AQP1-expressing oocytes was not different from that of native oocytes. All experiments with formamide and MeA were performed at least twice and gave similar results. There were no seasonal variations in the uptakes.

For each type of aquaporin, we can compare P_{NH3}, P_{form} and P_{MeA} since the data are obtained from oocytes with compatible levels of expression as estimated from the L_p. We conclude that AQP8, AQP9, AQP3 and TIP2;1 are permeable to formamide, with permeabilities around 10^{-6} cm/s, 20–50 times smaller than the corresponding P_{NH3}. P_{MeA} for AQP8, AQP9, and TIP2;1 is about 100 times lower than P_{NH3}; AQP3 is also permeable to MeA but with an even smaller permeability.

Reflection coefficients (σ) for hydrophilic substances

To determine whether small hydrophilic molecules interfere with water in the aqueous pore, we compared the shrinkage that resulted from an osmotic challenge with an impermeable osmolyte with that obtained with the test molecule [30] (Eqs. 2, 3). Oocytes were exposed to bathing solutions to which 20 mosm/l of either mannitol, urea, glycerol, acetamide or formamide had been added. Most aquaporins are impermeable to mannitol except for AQP9 [38, 39]. The larger molecule sucrose, however, had the same osmotic effects as mannitol in AQP9; consequently σ for mannitol is equal to σ for sucrose and can be assumed to be 1. The σ values are shown in Table 3. For AQP8, AQP9, AQP3 and TIP2;1-expressing oocytes, σ for formamide was much reduced (0.1–0.4). This suggests that formamide permeates the aqueous pore in agreement with the radiotracer data above.

Effects of NH_4Cl in unclamped oocytes

The membrane potential E_m of unclamped oocytes was recorded during abrupt isosmotic replacements of Na^+

Table 2 Permeabilities for methylammonium (P_{MeA}) and formamide (P_{form}). Experiments as in Fig. 2. The permeabilities for AQP9, AQP3, TIP2;1, and AQP1 were based on radiotracer uptakes of 30 s, except P_{MeA} for AQP9, which was based on a 60-s uptake. Means ± SE, (n)

Permeability (×10^{-7} cm/s)	AQP8	AQP9	AQP3	TIP2;1	AQP1	Native
P_{MeA}	5.3 ± 0.3* (16)	7.8 ± 0.8* (4)	2.4 ± 0.2 (5) NS	4.0 ± 0.3* (5)	2.3 ± 0.7 (5)	2.3 ± 0.5 (10)
P_{Form}	29.8 ± 1.3* (14)	27.7 ± 1.6* (5)	30.1 ± 0.1* (5)	34.0 ± 0.3* (5)	11.6 ± 0.3 (5)	14.6 ± 0.3 (15)

*$P < 0.05$ vs. native oocytes

Table 3 Reflection coefficient (σ) for osmolytes in oocytes expressing AQP8, AQP9, AQP3, TIP2;1, or AQP1. Data for AQP1 and AQP3 are from [30, 47] σ for the native oocyte membrane was 1 for mannitol, urea, acetamide and formamide; for glycerol, it was 1–0.9 [30, 47]. Means ± SE, (n)

Aquaporin	Mannitol	Urea	Glycerol	Acetamide	Formamide
AQP8	1	1.01 ± 0.04 (14)	0.97 ± 0.06 (14)	0.97 ± 0.04 (14)	0.20 ± 0.04 (14)
AQP9	1[a]	0.44 ± 0.07 (15)	0.44 ± 0.08 (14)	0.34 ± 0.05 (13)	0.30 ± 0.09 (12)
AQP3	1	1.00 ± 0.04 (15)	0.24 ± 0.02 (15)	0.72 ± 0.06 (15)	0.38 ± 0.03 (15)
TIP2;1	1	1.20 ± 0.07 (7)	1.06 ± 0.06 (7)	1.07 ± 0.09 (7)	0.09 ± 0.04 (7)
AQP1	1	0.98 ± 0.04 (15)	0.81 ± 0.01 (25)	0.94 ± 0.03 (18)	1.02 ± 0.03 (13)

[a] σ for mannitol is assumed to be 1, as the osmotic effects of mannitol and sucrose were not significantly different

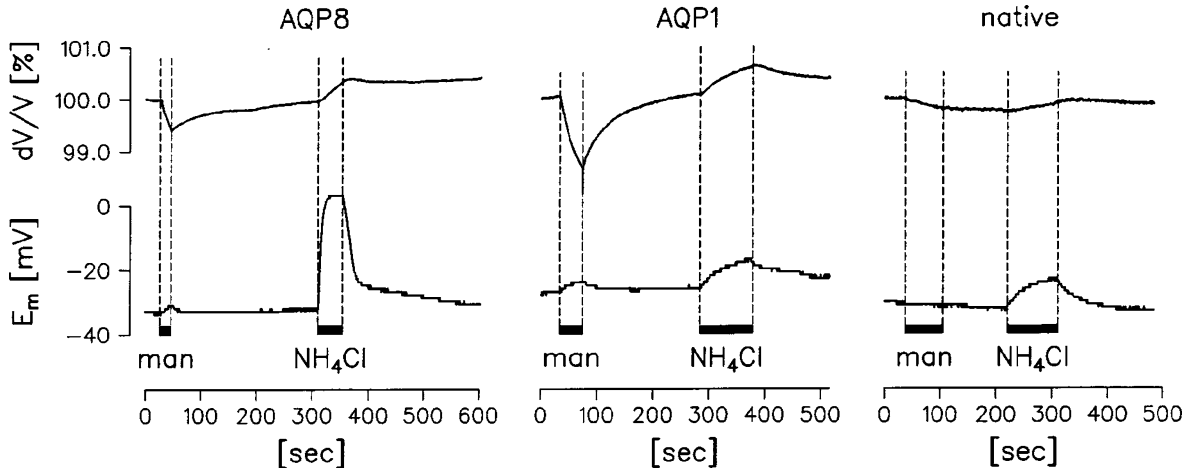

Fig. 3 The effects of NH_4^+ on membrane potential E_m and volume (V) in unclamped oocytes. The L_p of the oocytes was measured by the abrupt hyperosmolar addition of 20 mosm/l mannitol (*man*). After this, the effects of the isosmotic addition of 20 mM NH_4^+ (replacing Na^+) at pH of 7.4 were tested. Data for oocytes expressing AQP8, AQP9, AQP3, AQP1, and TIP2;1 are compared with those of native oocytes in Table 4

by NH_4^+ (20 mM) at pH_e 7.4. This induced a fast and large depolarization of E_m in oocytes expressing AQP8, AQP9, TIP2;1, and AQP3, while the effects on AQP1-expressing and native oocytes were much smaller (see Fig. 3, Table 4). The effects were most pronounced for AQP8 where E_m was virtually abolished in about 10 s. For AQP9, AQP3 and TIP2;1, the depolarization was somewhat smaller, E_m was halved in around 30 s. For both AQP1 and the native oocytes, the depolarizations were small, less than 10 mV, and took about 100 s to complete. The initial rate of depolarization and L_p are compared in Table 4. The slow depolarization observed for AQP1-expressing oocytes was not a result of low expression levels as judged from the L_p. The oocytes swelled during the NH_4Cl-induced depolarization (Fig. 3). The AQP8-expressing oocytes swelled initially by 140 ± 12 pl/s ($n = 4$) and the swelling began precisely at the onset of the depolarization. For the AQP1-expressing oocytes, the swelling was delayed by 9 ± 2 s ($n = 5$) relative to the depolarization and its maximal rate was 83 ± 7 pl/s ($n = 8$). For native oocytes swelling was delayed by 18 ± 2 s ($n = 8$) and its maximal rate was 29 ± 9 pl/s ($n = 9$). To study these electrical phenomena and associated volume movements under more well-defined conditions, oocytes were subjected to voltage clamp.

Clamp currents (I_C) induced by NH_4Cl in AQP8-expressing oocytes

The NH_4^+ conductance induced by NH_4Cl was studied under voltage-clamp conditions for AQP8-expressing oocytes. Oocytes were clamped to −50 mV in control bathing solutions and exposed abruptly to NH_4^+ (replacing Na^+) at different pH_e for 60 s (Fig. 4). In AQP8-expressing oocytes, 5 mM NH_4^+ initiated inwards clamp currents (I_C) that increased with a time constant of about 10–20 s and were 90% complete in 60 s (Fig. 4a). The induced currents were virtually absent for pH_e below 6.8, above 7.1 they increased with pH_e (i.e. with increasing $[NH_3]$). I_C was not affected if all Na^+ and K^+ in the external solution were replaced by choline ions, and there was no I_C when methylammonium ($CH_3NH_3^+$) replaced NH_4^+, and 20 mM at pH_e 7.4 was tested. The L_p of the AQP8-expressing oocytes was not dependent on pH_e (data not shown). The effects of NH_4^+ in native oocytes were small and only became apparent at $pH_e > 7.7$ (Fig. 4b). The difference between I_C obtained in the AQP8-expressing and in the native oocytes is given in Fig. 4c; the magnitude of each current was measured after 60 s. The difference current, which results from the insertion of the AQP8, depended on pH in a sigmoidal fashion. It was half-saturated at around pH_e 7.4 and fully saturated at around pH_e 7.8, with a magnitude of about

Table 4 Resting membrane potential (E_m) and initial rate of depolarization (d E_m/d t) of aquaporin-expressing oocytes in response to isosmotic addition of 20 mM NH_4^+ at pH 7.4 (see Fig. 3). Means ± SE, (n)

	AQP8	AQP9	AQP3	TIP2;1	AQP1	Native
E_m (mV)	32.8 ± 4 (5)	23.8 ± 1 (6)	35.6 ± 5 (5)	31.2 ± 3 (6)	23.4 ± 1 (5)	35.3 ± 4 (7)
d E_m/d t (mV/s)	4.1 ± 0.7* (5)	2.5 ± 0.6* (6)	0.87 ± 0.1* (5)	1.0 ± 0.08* (11)	0.29 ± 0.02 (5)	0.35 ± 0.03 (7)
L_p [$\times 10^{-5}$ cm s^{-1} (osm l^{-1})$^{-1}$]	7.2 ± 0.52 (5)	1.5 ± 0.16 (6)	5.9 ± 0.41 (5)	9.8 ± 0.38 (7)	6.8 ± 0.36 (9)	0.40 ± 0.01 (9)

*$P < 0.02$ vs. AQP1-expressing and native oocytes

200 nA. Similar results were obtained with longer-lasting currents, for instance 150 s instead of 60 s (Fig. 4d). Such long-lasting currents, particularly at high pH_e, required recovery times of 5 min, probably due to significant changes in intracellular concentrations.

To establish whether the I_C resulted from the expression process as such or from the higher L_p, we performed experiments with AQP1-expressing oocytes (Fig. 4e). These had L_p values similar to the AQP8-expressing oocytes (for values see the figure legends). The AQP1-expressing oocytes, however, had I_C values as low as those of native oocytes.

The inhibitor $HgCl_2$ (0.3 mM) initiated progressive depolarization of 1–2 mV/min in native oocytes (four oocytes). This agrees with previous findings in both native and AQP-expressing oocytes [30]. $HgCl_2$ is therefore not useful in voltage-clamp experiments.

Fig. 4a–e Clamp currents (I_C) induced by NH_4^+ as a function of external pH (pH_e). **a** An AQP8-expressing oocyte was clamped to −50 mV and 5 mM NH_4^+ added isosmotically (replacing Na^+) for 60 s to the bathing solution (*black bars*). Results at pH_e 7.1–8.0 are shown. **b** As in **a**, but with a native oocyte. **c** I_C from five AQP8-expressing oocytes (*open squares*) and five native oocytes (*nat*, *open circles*). The test solutions contained 5 mM NH_4^+ at pH_e 6.8–8.6, the corresponding [NH_3] are given on the *abscissa*. The difference between the data from the AQP8-expressing oocyte and those of the native oocyte was fitted to a sigmoidal function that saturated at around pH 7.7 (*filled triangles*). The L_p of the AQP8-expressing oocytes was 7.1 ± 0.8 ($n = 5$)and $0.33 \pm 0.02 \times 10^{-5}$ cm s^{-1} (osm $l^{-1})^{-1}$ ($n = 4$) for the native oocytes. **d** Long-term effects of isosmotic application of 5 mM NH_4Cl (pH_e 7.4). **e** NH_4^+-induced I_C in AQP1-expressing and native oocytes as a function of pH_e. The I_C for the AQP1-expressing and native oocytes were identical, the oocyte L_ps were the same as those of Fig. 5

Steady-state clamp currents (I_C) as a function of clamp voltage (V_C) for AQP8-expressing oocytes

To investigate the pH_e and voltage dependence of the conductance induced by NH_4^+, oocytes were bathed for 60 s in solutions containing 5 mM NH_4^+ at various pH_e (experiments as above). At this point, the clamp voltage was stepped from the holding voltage (−50 mV) to a series of seven voltages ranging from +50 mV to −100 mV, in steps of 25 mV lasting 85 ms (Fig. 5a). At each pulse, the steady-state I_C was measured after, typically, 10 ms. In AQP8-expressing oocytes, the I_C/V_C curves obtained at pH_e 7.4 showed inwards rectification. At higher pH_e, the reversal potentials decreased with increasing pH_e, at pH_e 8.6 it was 18.1 ± 1.1 mV ($n = 5$).

The current induced by NH_4^+ saturated at high pH_e (Fig. 4c). To determine whether it was the current or the conductance that saturated, we calculated the slope conductance from the increment in I_C observed for changes in V_C from −75 mV to −50 mV ($g = \Delta I_C$/25 mV). Values are plotted as a function of pH_e (or [NH_3]), the control solution is taken as 0 mM NH_3 (Fig. 5c). Values from AQP1-expressing oocytes are included. We conclude that it is the conductance of the NH_3-induced NH_4^+ transport system that saturates at higher pH_e; accordingly the transport rate can be increased by increasing the electrical gradient.

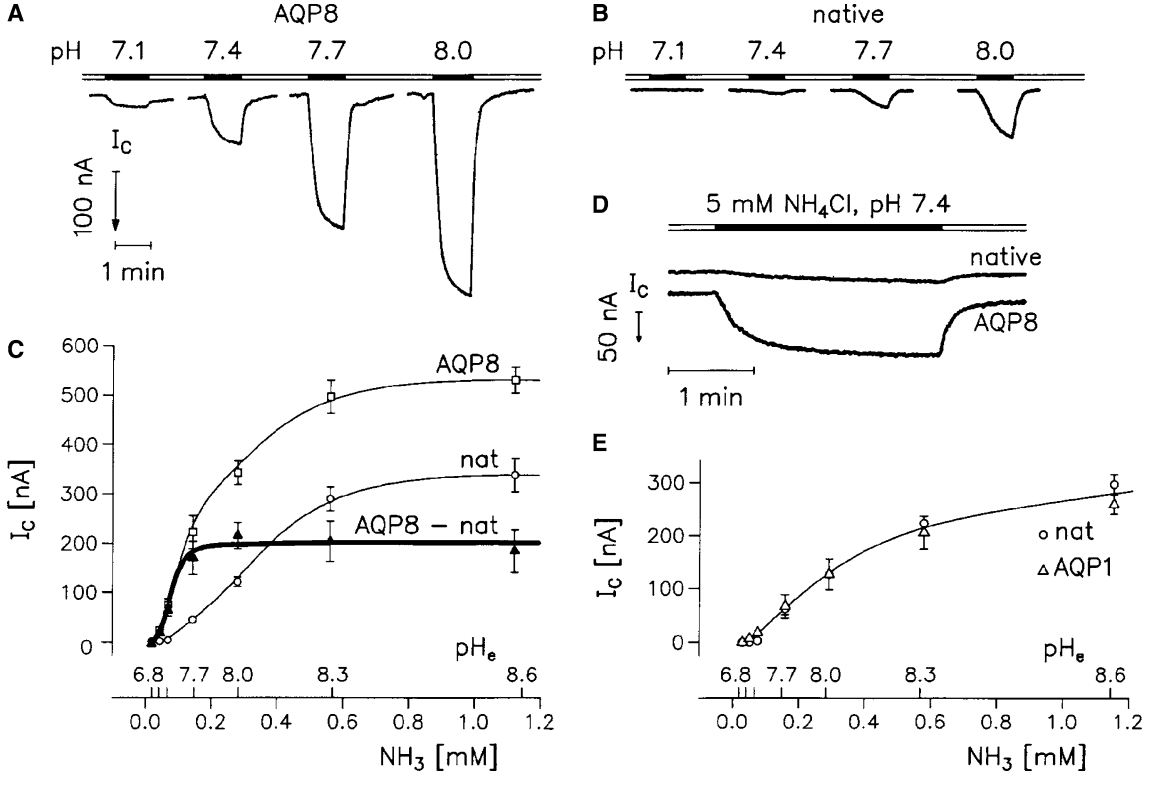

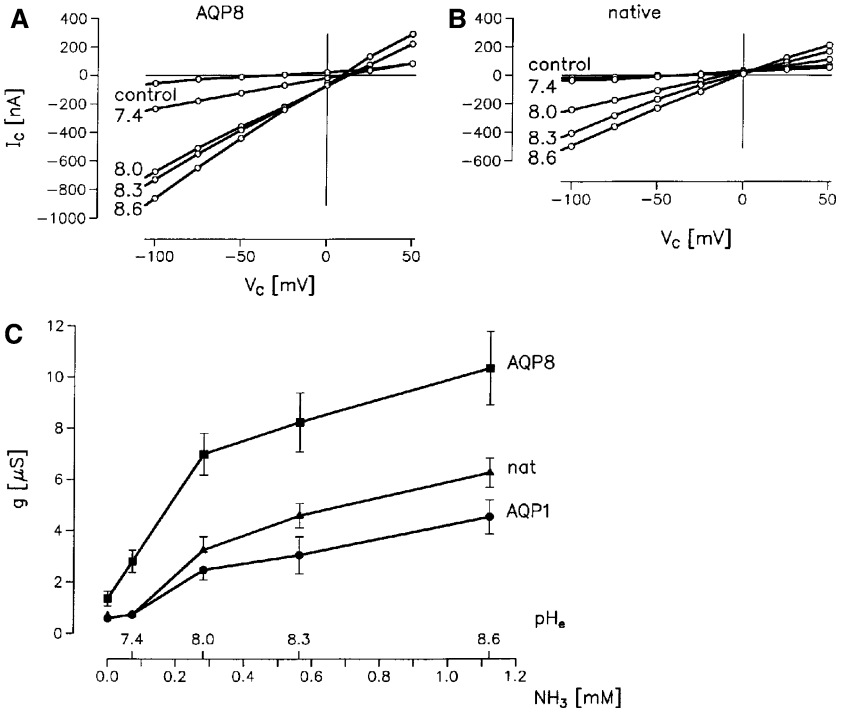

Fig. 5a-c Steady-state I_C and conductances as a function of clamp voltage (V_C). Oocytes were bathed in control solution or for 60 s in solutions in which 5 mM NH_4^+ replaced Na^+ at various pH_e (see Fig. 4). V_C was stepped from a holding voltage of −50 mV to a series of seven voltage pulses ranging from +50 mV to −100 mV, in steps of 25 mV lasting 85 ms. At each pulse, the steady-state I_C was obtained after about 10 ms. **a** AQP8-expressing oocyte bathed in control solution and in solutions with 5 mM NH_4^+ at pH_e 7.4, 8.0 or 8.6. **b** A native oocyte. **c** Slope conductances (g) based on the increment in I_C associated with increases in V_C from −75 mV to −50 mV. Values are plotted as a function of pH_e (or $[NH_3]$), the control solution is taken as 0 mM NH_3. L_p values were: AQP8-expressing oocytes 8.0 ± 0.3 (n = 9),native oocytes 0.4 ± 0.02 (n = 4), AQP1-expressing oocytes $6.9 \pm 0.7 \times 10^{-5}$ cm s^{-1} (osm l^{-1})$^{-1}$ (n = 5). There was no significant difference between data from AQP1-expressing and native oocytes. There was no significant difference between the values for AQP8-expressing, AQP1-expressing, and native oocytes in control solutions. In **a** and **b**, the I_C/V_C curves returned to control values at return to control bathing solution (not shown)

Volume changes during NH_4Cl-induced clamp currents

To determine whether I_C reflected the influx of positive ions into or the efflux of negative ions out of the oocyte, we recorded oocyte volume changes and I_C simultaneously in experiments as those described in Fig. 4. Two examples from an AQP8-expressing oocyte obtained at different pH_e are shown in Fig. 6a. The initial rates of volume changes as a function of pH_e are summarized in Fig. 6d. For AQP8-expressing oocytes, the initial rate of swelling increased with pH_e increasing from 6.8 to 7.7, after which there was a slight decrease with pH_e. For the experiment shown in Fig. 6a, I_C at pH_e 7.4 was about 50 nA and the rate of volume increase declined with time. At pH 8.6, the I_C was associated with a linear increase in volume. There seemed to be two types of swelling: (1) In the absence of any significant I_C (at a pH_e of 6.8), there was a marked swelling of about 50 pl/s. Given the L_p of the AQP8-expressing oocytes (see legend, Fig. 6), it can be calculated that the rate of swelling corresponds to an osmotic challenge of 3 mosm/l. In other words, the 5 mM NH_4Cl, which contributes 10 mosm/l to the bathing solution osmolarity, is seen as about only 7 mosm/l by the oocyte. Accordingly, the apparent σ for NH_4Cl is significantly less than 1, indicating that NH_4Cl interferes with water in the aqueous channel (Eq. 3). (2) It can be calculated [49] that the additional rate of swelling observed at higher pH_e corresponds to the I_C if it is assumed that the current results from NH_4^+ ions entering the oocyte. Swelling was the same if all Na^+ and K^+ in the bathing solutions were replaced by choline ions.

Figure 6d shows that AQP8-expressing oocytes swelled markedly during exposure to 5 mM NH_4^+, as indicated by the positive values of d V/d t. AQP1-expressing oocytes exhibited minor degrees of swelling at lower pH and shrinkage at higher pH. The volume changes observed in AQP1-expressing oocytes were thus different from those observed in AQP8-expressing oocytes (Fig. 6b,d). For pH_e below 8.0, initial volume changes were absent or indicated a small swelling. For $pH_e > 8.0$, the oocytes initially shrank, followed some 50 s later by swelling. Probably, the clamp current arises as a result of Cl^- transport out of the cell (shrinkage) in combination with inwards transport of NH_4^+. The L_p values of the AQP1-expressing oocytes were similar to those of the AQP8-expressing oocytes. Native oocytes showed little or no change in volume with NH_4^+ exposure under clamp conditions (Fig. 6c,d). This is probably due to the fact that the L_p of these oocytes are about 20 times lower than those of the AQP8- and

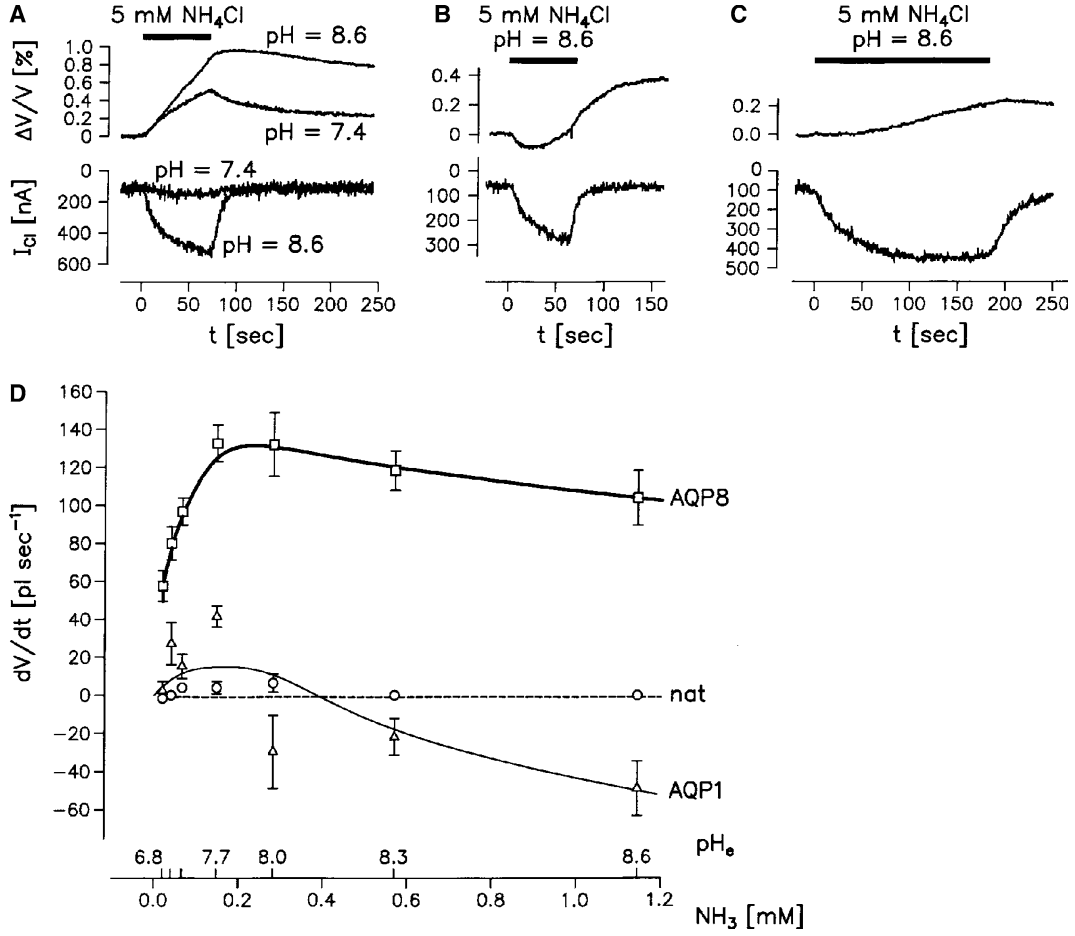

Fig. 6a–d Volume changes and NH_4^+-induced I_C. **a** Relative volume changes (d V/V) of an AQP8-expressing oocyte in experiments as those shown in Fig. 4 with exposure to 5 mM NH_4^+ at pH_e 7.4 and 8.6. L_p of the AQP8-expressing oocyte was 4.3×10^{-5} cm s^{-1} (osm $l^{-1})^{-1}$. **b** AQP1-expressing oocyte exposed to 5 mM NH_4^+ at pH_e 8.6; the oocyte initially shrank. L_p of the AQP1-expressing oocyte was 6.0×10^{-5} cm s^{-1} (osm $l^{-1})^{-1}$. **c** Native oocyte exposed to 5 mM NH_4^+ at pH_e 8.6. The volume change was initially zero followed by a slow swelling. Note the different *volume scales* in **b** and **c** compared with **a**. **d** Summary of the initial rate of change in volume (d V/d t). *Open squares*: AQP8-expressing oocytes, *open triangles*: AQP1-expressing oocytes, *open circles*: native oocytes. L_p of the AQP8-expressing oocytes was 7.1 ± 0.8 ($n=5$), of the AQP1-expressing oocytes 6.6 ± 0.4 ($n=8$) and of the native oocytes $0.38\pm0.02\times10^{-5}$ cm s^{-1} (osm $l^{-1})^{-1}$ ($n=4$)

AQP1-expressing oocytes. Even if the clamp currents and ionic and osmotic changes were similar in AQP1-expressing and native oocytes, the volume changes observed in the native oocytes would be 20 times smaller.

Comparison between clamp currents and volume changes in oocytes expressing AQP9, AQP3, TIP2;1, and AQP8

In analogy to the AQP8-expressing oocytes, AQP9-, AQP3- and TIP2;1-expressing oocytes supported significant NH_4^+-dependent I_C. The data obtained on isosmotic exposure to 5 mM of NH_4^+ at pH 7.4 are compared in Fig. 7a (experiments as in Fig. 4). AQP9-expressing oocytes were as effective as AQP8-expressing ones while those expressing AQP3 or TIP2;1 had slightly smaller I_C. The I_C of AQP1- and tip2;1-expressing and native oocytes were all small. Similar data were obtained with 10 and 20 mM NH_4^+ at pH_e 7.4, (data not shown).

The initial volume changes associated with I_C at 5 mM NH_4^+ at pH 7.4 for AQP8-, AQP9-, AQP3-, and TIP2;1-expressing oocytes were significantly larger than those observed for native, AQP1- and tip2;1-expressing oocytes (experiments as in Fig. 6). To correct for differences in L_p, the rate of swelling was normalised relative to the respective L_p (Fig. 7b). The volume changes observed for AQP9 and AQP3 were only half those of AQP8 and TIP2;1.

Intracellular changes in pH

Intracellular pH (pH_i) was measured with ion-selective, double-barrelled microelectrodes, the tips of which were inserted to a depth of about 100 μm into the oocytes. When bathed in control solutions (pH_e 7.4) under steady-state conditions, pH_i was 7.1–7.3 in both native and aquaporin-expressing oocytes (Table. 5). There were no

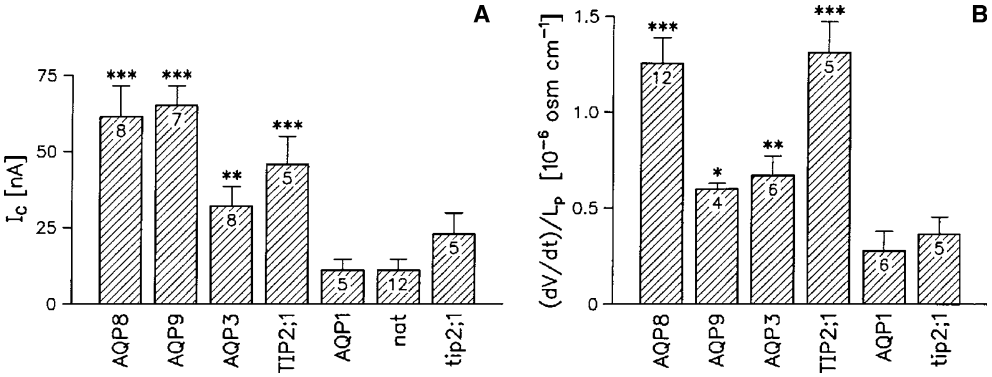

Fig. 7a,b Comparison between oocytes expressing AQP8, AQP9, AQP3, TIP2;1, tip2;1, or AQP1 and native oocytes. **a** Effect of isosmotic exposure to 5 mM NH_4^+ at pH_e of 7.4 under voltage-clamp conditions, $V_C = -50$ mV. I_C was measured after 60 s (Fig. 4a,b). I_C for TIP2;1 was also larger than that for the mutated tip2;1 ($P < 0.03$). **b** Corresponding initial rates of volume changes (see Fig. 6d) relative to the L_p of each oocyte. L_ps were AQP8: 7.1 ± 0.3 ($n = 8$); AQP9: 1.3 ± 0.13 ($n = 7$); AQP3: 5.1 ± 0.3 ($n = 8$); TIP2;1: 7.0 ± 0.5 ($n = 5$); tip2;1: 7.9 ± 0.6 ($n = 5$); AQP1: 5.6 ± 0.9 ($n = 3$); native: $0.36 \pm 0.02 \times 10^{-5}$ cm s^{-1} (osm l^{-1})$^{-1}$ ($n = 11$) (*$P < 0.05$, **$P < 0.01$. ***$P < 0.003$ vs. nat, AQP1 and tip2;1)

differences among the various aquaporins. When exposed abruptly to isotonic solutions containing 20 mM NH_4Cl at pH_e 7.4, pH_i initially exhibited a peak of alkalinization of no more than 0.3 pH units. This was followed after 10–60 s by acidification which achieved maximal rates in the range 0–0.2 pH/min; the largest values were obtained for AQP8-expressing oocytes (0.16 ± 0.03 pH/min, $n = 6$). The response in pH_i, however, was dependent on the position of the tip of the electrode with smaller changes observed closer to the centre of the oocytes. After exposure to NH_4Cl, pH_i was around 0.2 pH units more acidic in the centre than just below the membrane.

Discussion

We have shown above that the mammalian aquaporins AQP3, AQP8, AQP9 and the plant aquaporin TIP2;1 are permeable to NH_3, in agreement with our observations in the yeast expression system [21]. In addition, these aquaporins induce an NH_4^+ conductance when expressed in *Xenopus* oocytes. We will first discuss the permeability to NH_3 and then the question of whether the NH_4^+ conductance is a property of the aquaporin itself or whether endogenous mechanisms in the oocyte are activated by the influx of NH_3. Finally, we address the physiological relevance of our findings.

Amides permeate the aqueous pore of AQP8, AQP9, AQP3, and TIP2;1

Expression of these aquaporins increased the permeability to NH_3 and the larger amides methylammonium and formamide above that of native oocytes (Figs. 1, 2, Tables 1, 2). This agrees with the finding of a low σ for formamide (Table 3). According to conventional thermodynamics (Eq. 3), a low σ suggests that formamide permeates via the aqueous pore. AQP8-expressing oocytes swelled when exposed to isosmotic NH_4Cl even when there was no current flow, i.e. at low pH_e(Fig. 6d). This low σ for NH_4Cl suggests that NH_4Cl has access to the aqueous pore. It should be emphasized that the physical meaning of reflection coefficients is still under debate. A low σ may signify interaction between solvent and solute in the pore but not necessarily permeation [17].

In control experiments, expression of AQP1 or the mutant tip2;1 did not increase P_{NH3} above that of native oocytes (Table 1). Furthermore, formamide had a σ of 1 in AQP1-expressing oocytes and exposure to NH_4Cl produced only small volume changes (Fig. 6). This shows that the NH_3 permeability is not the result of the expression process per se, and that there is probably no NH_3 permeation via the interphase between the aquaporin and the lipid bilayer or via a central opening in a putative tetrameric assembly of the aquaporins; AQP1 has been shown to form tetrameric assemblies [31].

The data show that the width of the pore of AQP8, AQP9, AQP3, and TIP2;1 is functionally larger than that of AQP1 or tip2;1. These differences should be viewed in relation to highly significant differences in the

Table 5 Intracellular pH (pH_i) and membrane potential (E_m) under control conditions. Δ pH_i is the extra acidity in the centre relative to just inside the membrane after exposure to NH_4^+ (see text). Means ± SE, (n)

	AQP8	AQP9	AQP3	TIP2	AQP1	Native
E_m (mV)	−27.8 ± 4.0 (5)	−25.3 ± 1.7 (7)	−35.2 ± 1.2 (24)	−26.9 ± 2.1 (8)	−26.4 ± 1.8 (7)	−40.8 ± 2.5 (19)
pH_i	7.31 ± 0.06 (5)	7.21 ± 0.05 (7)	7.06 ± 0.02 (24)	7.16 ± 0.07 (8)	7.12 ± 0.05 (7)	7.13 ± 0.12 (19)
Δ pH_i in centre	−0.11 ± 0.07 (5)	−0.19 ± 0.03 (7)	−0.19 ± 0.03 (4)	−0.11 ± 0.03 (7)	−0.24 ± 0.01 (4)	−0.17 ± 0.03 (17)

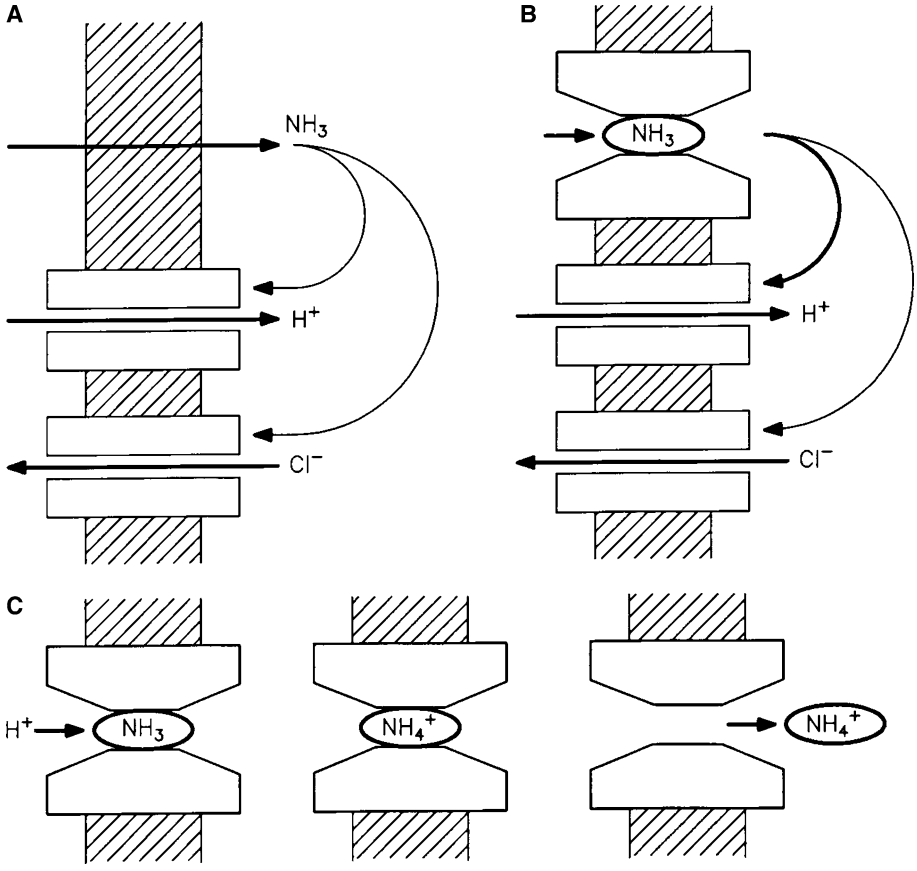

Fig. 8a–c Working hypothesis for the NH_3-induced NH_4^+ conductance observed under voltage-clamp conditions. *a* In native and AQP1-expressing oocytes, NH_3 enters via the lipid bilayers and stimulates endogenous channels for H^+ (for example in the form of NH_4^+) and for anion transport (Cl^-). At high external [NH_3] the Cl^- conductance dominates, as seen from the initial shrinkage of the oocyte (Fig. 6b). For oocytes expressing AQP8, AQP9, AQP3, or TIP2;1, there are two possible models: In the first (**b**) NH_3 enters rapidly via the aquaporin and stimulates the endogenous channels. To explain the associated net entry of osmotically active particles (i.e. swelling of the oocyte, Fig. 6a), the model requires that NH_3 stimulates the entry of H^+ (NH_4^+) more efficiently than the exit of Cl^-; one possibility would be that the aquaporin co-localizes with the pathway for H^+. In the second model (**c**) both NH_3 and H^+ transport takes place via the aquaporin. NH_3 in the pore acts as a binding site for H^+ from the external solution. In contrast to water, NH_3 may react with H^+ through the aqueous pore (see text). NH_4^+ leaves the pore towards the side with the most negative electrochemical potential, i.e. the intracellular compartment

primary structures of AQP1 and the ammonium-permeable aquaporins. For TIP2;1 and tip2;1, the different transport properties for ammonia relate to the $I^{184}H$ and $G^{193}C$ substitution in the pore region [21]. These substitutions reduced P_{NH3} but, most importantly, did not affect the L_p.

NH_3-gated NH_4^+ conductance

Expression of the NH_3-permeable aquaporins AQP8, AQP9, AQP3 or TIP2;1 increased the NH_4^+ conductance of the oocytes above that of native oocytes while expression of AQP1 did not. Expression of tip2;1 increased the conduction slightly but not significantly (Fig. 7).

In AQP8-, AQP3-, AQP9- and TIP2;1-expressing oocytes, the inward clamp currents are most probably carried by NH_4^+ for the following reasons. (1) The currents were associated with the swelling of the oocyte (Fig. 6), which shows that osmotic active particles enter the oocyte. (2) Currents were not affected by removal of Na^+ and K^+ from the bathing solution but (3) were abolished when MeA^+ replaced NH_4^+ (data not shown). (4) The NH_4^+-dependent clamp current required a certain concentration of NH_3. It was absent at pH_e more acidic than 6.8 (Fig. 4c) showing that the conduction mechanisms do not accept H^+ per se. Only at around pH_e of 7.1 did conduction become significant, and it saturated at pH_e 7.8. (5) Any current component carried by anions must be small compared with the effect seen in AQP1-expressing oocytes (below). The current in the microelectrode providing the clamp current does not contribute to the intracellular osmolarity since it is composed of equal and opposite fluxes of K^+ and Cl^- [49].

In AQP1-expressing oocytes, the effects induced by NH_4Cl were similar to those seen in native oocytes (Fig. 4e), but differed in several aspects from those observed for the ammonia-permeable aquaporins. (1) The clamp currents were smaller and took a longer time to develop (compare Fig. 4a,b). (2) In the initial phases, at

low pH_e, the currents were associated with no or little change in oocyte volume; at high pH_e, the oocytes even shrank (Fig. 6b–d). These changes were visible in the AQP1-expressing oocytes due to their high L_p. Most likely, the clamp current results from a combination of an inwards cation flux and an outwards anion flux (Fig. 8a). The cation flux is probably carried by NH_4^+ since the oocytes acidify with prolonged exposure to NH_4Cl [3–6, 9, 26, 33, 39]. The outwards flux of anions, probably Cl^-, dominates the initial phases at high pH_e and as a consequence, osmotic active particles are lost from the oocyte and it shrinks.

Against this background, we discuss, in the following, two working hypotheses for the NH_4^+ transport induced by the ammonia-permeable aquaporins (Fig 8). In the first model, the ammonia-permeable aquaporins transport only NH_3. The influx of NH_3 and the associated changes in pH_i open endogenous channels for H^+ (for example in the form of NH_4^+) and for Cl^- transport (Fig. 8b). In the second model, the ammonia-permeable aquaporins mediate both the NH_3 and the H^+ transport in the form of a NH_4^+ current (Fig. 8c).

The first model (Fig. 8b) cannot account for several experimental findings and would require additional assumptions to work. Under clamp conditions, oocytes that express ammonia-permeable aquaporins swell rapidly when exposed to NH_4Cl, while AQP1-expressing oocytes swell only a little or may even shrink (Figs. 6, 7). Apparently, the efflux of anions plays a significant role in the AQP1-expressing oocytes, while the inwards NH_4^+ current dominates in the oocytes that express ammonia-permeable aquaporins. If the ammonia-permeable aquaporins simply increased the influx of NH_3, we would expect these oocytes to shrink in analogy to the AQP1-expressing oocyte. If we make the additional assumption that the ammonia-permeable aquaporins are expressed in close proximity to the endogenous channel for H^+, this could give rise to a specific and potent stimulation of the H^+ pathway compared with that of the pathway for anions. Even so, the model would not explain the low σ for NH_4Cl observed at low [NH_3] (Fig. 6d). Isosmotic replacement of 5 mM of NaCl by NH_4Cl at pH_e 6.8 induced cell swelling. Apparently, NH_4Cl is not as effective osmotically as NaCl, suggesting that NH_4Cl has direct access to the aqueous pathway of the ammonia-permeable aquaporins (Eq. 3).

The second model (Fig. 8c) suggests that NH_3 present in the pore of an ammonia permeable aquaporin can act as a site for H^+ ions and that the NH_4^+ formed proceeds to the side with the most negative potential. This NH_4^+ current would explain directly the NH_4Cl-induced swelling; at acidic pH_e where there was no current flow, swelling would arise as a result of the low σ (Fig. 6d). The problem with this model is to explain how a positive charge can permeate the channel. In the case of H_2O transport, it is well known that transport of H^+ is abolished. The string of hydrogen bonds among adjacent H_2O molecules does not stretch throughout the channel since the H_2O molecule in the NPA region of the channel is forced to orientate its H^+ bonds towards the protein and away from the neighbouring H_2O [31]. Now, NH_3molecules do not share the dipole properties of H_2O molecules and may behave differently in the NPA region: the NH_3 molecule may retain its ability to take up and release H^+ anywhere in the aqueous pore. Since the transport of NH_3 into the channel is a rate-limiting step, this model complies with the low NH_4^+ conductance per aquaporin, estimated below.

The unit transport capacity for NH_4^+ induced by AQP8, AQP9, AQP3, and TIP2;1 is much lower than that of ordinary ion channels, as can be seen from a rough estimate: the L_p of the aquaporin-expressing oocytes is about 3×10^{-3} cm/s. With a unit L_p of around 3×10^{-14} cm^3/s (for a review see [11]), the oocytes must express about 10^{11} copies of the aquaporin per cm^2. This is 5–10 times lower than the estimated density of AQP1 in human red cells [13]. The aquaporins conduct up to 1,000 nA/cm^2 (Figs. 5, 7) equivalent to a turn-over of about 50/s. This rate is much lower than that of H_2O transport, which is around 10^5/s for an osmotic gradient of 1 mosm/l. The conductance per unit surface area (cm^2) of oocyte is about 10^{-5} S cm^2 (Fig. 5) equivalent to a unit conductance of 10^{-16} S, far below of that of ordinary ion channels. Diffusion of NH_3 towards and binding to a binding site in the channel might determine the (slow) rate-limiting step of the transport process.

Measurements of pH_i

In agreement with previous findings [4, 5, 9, 26, 33, 39], all types of oocytes initially exhibited an increase in pH_i when exposed to NH_4Cl. This was variable both in magnitude and duration and was followed by acidification resulting from the entry of NH_4^+. This acidification was most pronounced for AQP8. Further quantitative evaluation was difficult since the pH_i changes were not uniform throughout the oocyte. Several factors must be considered: The intracellular distribution of NH_3 and NH_4^+ could be different during the non-steady-state influx of NH_4^+/NH_3. Two-thirds of the oocyte volume is taken up by structures that are osmotically inaccessible in the short term, such as yolk platelets, vitelline vesicles and other organelles [49]. These structures may be accessible to NH_3, but not to NH_4^+. This would explain why both pH_e and pH_i acidify during exposure to NH_4Cl; the tip of the microelectrode is in the aqueous part of the volume, while the NH_3 that should have balanced the NH_4^+ is taken up by the organelles. Different rates of diffusion of NH_3 and NH_4^+, as well as impeded diffusion of intracellular buffers, may also contribute [42, 45].

Physiological relevance

Ammonium (NH_4^+) is potentially toxic, yet is an essential component in amino acid metabolism. As a

consequence, transport of NH_4^+ has to be directed precisely, the transport rate controlled and plasma concentrations kept low. In these respects, the aquaporin-mediated transport of NH_3/NH_4^+ has the advantage of being located and adjusted to the requirements of the cell or organelle in question via the expression level of the aquaporins. In this sense, AQP8, AQP9, and AQP3 belong to the group of ammonium-transporting proteins, which in mammals include the Rhesus family [3, 23, 26, 32].

AQP8 shows a wide range of tissue expression. For most cells, it is located predominantly intracellularly in organelles [7, 10, 12, 14, 19, 36], which would suggest a role in the metabolism of amino acids. In the liver, for example, AQP8 can be found in the mitochondria of hepatocytes [12], suggesting a direct role for the uptake of NH_4^+ to supply the urea cycle. Mitochondria have large negative membrane potentials of about −150 mV [34], which would facilitate inwards transport.

AQP9 is found in the hepatocyte plasma membrane facing the sinusoids [8, 19, 36]. In humans, the portal venous blood (about 20 ml/s) contains 0.2–0.5 mM NH_4^+ originating from the intestine. This adds to the ammonium produced inside the hepatocyte [15, 16]. We suggest that NH_4^+ is taken up from the blood into the periportal hepatocytes via AQP9 from where it may enter the (electro-negative) mitochondrion. During starvation, AQP9 expression increases [8] in accordance with this hypothesis. Urea produced in the urea cycle may leave the cell again via AQP9 [8, 41].

AQP3 has a wide tissue distribution [2]. In the kidney, AQP3 has been found in the basolateral membrane of principal cells in cortical and outer medullary collecting ducts [35, 38]. Hence, AQP3 could play a direct role in the final steps of acid secretion via NH_4^+, which takes place across the collecting duct epithelium [24]. AQP3 knockout mice have a marked urinary concentration defect with severe polyuria [27, 43]. It is to be expected that these mice have tubular acidosis and therefore reduced capacity for concentrating the final urine.

Acknowledgements The authors are grateful for expert technical assistance from B. Lynderup, T. Soland and S. Christoffersen and for valuable discussions with Dr. E. Beitz. The study was supported by the Nordic Centre of Excellence Programme in Molecular Medicine, The Danish Research Council Veluxfonden, Øjenforeningen, Alice and Jørgen Rasmussens mindelegat and the Lundbeck Foundation to T.Z., SJVF (23-03-0103) to T.P.J and the Centro di Eccellenza di Genomica in campo Biomedico ed Agrario and Fondo per gli Investimenti della Ricerca di Base (RBAU01RANB).

Appendix

In aqueous solutions of NH_4Cl, NH_4^+ is present together with its conjugate base NH_3. Under equilibrium conditions, $NH_4^+ = NH_3 \times 10^{pK-pH}$ with pK = 9.25. Thus, for the external solution:

$$\frac{-\mathrm{dpH}}{2.3\mathrm{d}t} = \frac{\mathrm{dH}^+}{\mathrm{H}^+\,\mathrm{d}t} = \frac{-\mathrm{dNH_3}}{\mathrm{NH_3 d}t} + \frac{\mathrm{dNH_4}^+}{\mathrm{NH_4}^+\,\mathrm{d}t}. \quad (4)$$

Consequently, if the *relative* rate of influx of NH_3 is larger than that of NH_4^+, the external solution acidifies. With $dNH_3/dt = -P_{NH3} \times NH_3$ and $dNH_4^+/dt = -P_{NH4}^+ \times NH_4^+$, Eq. 4 becomes

$$\frac{-\mathrm{dpH}}{2.3\mathrm{d}t} = \frac{\mathrm{dH}^+}{\mathrm{H}^+\mathrm{d}t} = \mathrm{P_{NH3}} - \mathrm{P_{NH4}^+}. \quad (5)$$

In other words, if P_{NH3} is larger than P_{NH4+} the external solution will acidify. Note that P_{NH4+} incorporates electrical terms.

References

1. Ackerman MJ, Wickman KD, Clapham DE (1994) Hypotonicity activates a native chloride current in *Xenopus* oocytes. J Gen Physiol 103:153–179
2. Agre P, King LS, Yasui M, Guggino WB, Ottersen OP, Fujiyoshi Y, Engel A, Nielsen S (2002) Aquaporin water channels—from atomic structure to clinical medicine. J Physiol (Lond) 542:3–16
3. Bakouh N, Benjelloun F, Hulin P, Brouillard F, Edelman A, Chèrif-Zahar B, Planelles G (2004) NH_3 is involved in the NH_4^+ transport induced by the functional expression of the human Rh C glycoprotein. J Biol Biochem 279:15975–15983
4. Boldt M, Burckhardt G, Burckhardt BC (2003) NH_4^+ conductance in *Xenopus laevis* oocytes. III. Effect of NH_3. Pflugers Arch 446:652–657
5. Burckhardt B-C, Frömter E (1992) Pathways of NH_3/NH_4^+ permeation across *Xenopus laevis* oocyte cell membrane. Pflugers Arch 420:83–86
6. Burckhardt B-C, Burckhardt G (1997) NH_4^+ conductance in *Xenopus laevis* oocytes. Pflugers Arch 434:306–312
7. Calamita G, Mazzone A, Bizzoca A, Cavalier A, Cassano G, Thomas D, Svelto M (2001) Expression and immunolocalization of the aquaporin-8 water channel in rat gastrointestinal tract. Eur J Cell Biol 80:711–719
8. Carbrey JM, Gorelick-Feldman DA, Kozono D, Praetorius J, Nielsen S, Agre P (2003) Aquaglyceroporin AQP9: solute permeation and metabolic control of expression in liver. Proc Natl Acad Sci USA 100:2945–2950
9. Cougnon M, Bouyer P, Hulin P, Anagnostopoulos T, Planelles G (1996) Further investigation of ionic diffusive properties and of NH_4^+ pathways in *Xenopus laevis* oocyte cell membrane. Pflugers Arch 431:658–667
10. Elkjær M-L, Nejsum LN, Gresz V, Kwon T-H, Jensen UB, Frøkiær J, Nielsen S (2001) Immunolocalization of aquaporin-8 in rat kidney, gastrointestinal tract, testis, and airways. Am J Physiol 281:F1047–F1057
11. Engel A, Stahlberg H (2002) Aquaglyceroporins: channel proteins with a conserved core, multiple functions, and variable surfaces. Int Rev Cytol 215:75–104
12. Ferri D, Mazzone A, Liquori GE, Cassano G, Svelto M, Calamita G (2003) Ontogeny, distribution, and possible functional implications of an unusual aquaporin, AQP8, in mouse liver. Hepatology 38:947–957
13. Finkelstein A (1987) Water movement through lipid bilayers, pores and plasma membranes. Wiley-Interscience, New York
14. Garcia F, Kierbel A, Larocca MC, Gradilone SA, Splinter P, LaRusso NF, Marinelli RA (2001) The water channel aquaporin-8 is mainly intracellular in rat hepatocytes, and its plasma membrane insertion is stimulated by cyclic AMP. J Biol Chem 276:12147–12152

15. Häussinger D (1996) Physiological functions of the liver. In: Greger R, Windhorst U (eds) Comprehensive human physiology, Vol. 2. Springer, Berlin Heidelberg New York, pp 1369–1391
16. Häussinger D (1996) Zonal metabolism in the liver. In: Greger R, Windhorst U (eds) Comprehensive human physiology, Vol 2. Springer, Berlin Heidelberg New York, pp 1393–1402
17. Hill EA (1994) Osmotic flow in membrane pores of molecular size. J Membr Biol 137:197–203
18. Holm LM, Klaerke DA, Zeuthen T (2004) Aquaporin 6 is permeable to glycerol and urea. Pflügers Arch 448:181–186
19. Huebert RC, Splinter PL, Garcia F, Marinelli RA, LaRusso NF (2002) Expression and localization of aquaporin water channels in rat hepatocytes. J Biol Chem 277:22710–22717
20. Ishibashi K, Kuwahara M, Gu Y, Tanaka Y, Marumo F, Sasaki S (1998) Cloning and functional expression of a new aquaporin (AQP9) abundantly expressed in the peripheral leukocytes permeable to water and urea, but not to glycerol. Biochem Biophys Res Commun 244:268–274
21. Jahn TP, Møller ALB, Zeuthen T, Holm LM, Klaerke DA, Mohsin B, Kühlbrandt W, Schjoerring JK (2004) Aquaporin homologues in plants and mammals transport ammonia. FEBS Lett 574:31–36
22. Kedem O, Katchalsky A (1961) A physical interpretation of the phenomenological coefficients of membrane permeability. J Gen Physiol 45:143–179
23. Khademi S, O'Connell III J, Remis J, Robles-Colmenares Y, Miercke LJW, Stroud RM (2004) Mechanism of ammonia transport by Amt/MEP/Rh: structure of AmtB at 1.35 Å. Science 305:1587–1594
24. Knepper MA, Packer R, Good DW (1989) Ammonium transport in the kidney. Physiol Rev 69:179–249
25. Koyama Y, Yamamoto T, Kondo D, Funaki H, Yaoita E, Kawasaki K, Sato N, Hatekeyama K, Kihara I (1997) Molecular cloning of a new aquaporin from rat pancreas and liver. J Biol Chem 272:30329–30333
26. Ludewig U (2004) Electroneutral ammonium transport by basolateral rhesus B glycoprotein. J Physiol (Lond) 559:751–759
27. Ma T, Song Y, Yang B, Gillespie A, Carlson EJ, Epstein CJ, Verkman AS (2000) Nephrogenic diabetes insipidus in mice lacking aquaporin-3 water channels. Proc Natl Acad Sci USA 97:4386–4391
28. Ma T, Yang B, Verkman AS (1997) Cloning of a novel water and urea-permeable aquaporin from mouse expressed strongly in colon, placenta, liver and heart. Biochem Biophys Res Commun 240:324–328
29. Meinild A-K, Klaerke DA, Loo DDF, Wright EM, Zeuthen T (1998) The human Na^+ /glucose cotransporter is a molecular water pump. J Physiol (Lond) 508:15–21
30. Meinild A-K, Klaerke DA, Zeuthen T (1998) Bidirectional water fluxes and specificity for small hydrophilic molecules in aquaporins 0 to 5. J Biol Chem 273:32446–32451
31. Murata K, Mitsouka K, Hirai T, Walz T, Agre P, Heymann JB, Engel A, Fujiyoshi Y (2000) Structural determinants of water permeation through aquaporin-1. Nature 407:599–605
32. Nakhoul NL, Hamm LL (2004) Non-erythroid Rh glycoproteins: a putative new family of mammalian ammonium transporters. Pflugers Arch 447:807–812
33. Nakhoul NL, Hering-Smith KS, Abdulnour-Nakhoul SM, Hamm LL (2001) Transport of NH_3/NH_4^+ in oocytes expressing aquaporin-1. Am J Physiol 281:F255–F263
34. Nicholls DG, Ferguson SJ (1995) Bioenergetics 2 edn. Academic Press, London
35. Nielsen S, Frøkier J, Marples D, Kwon T-H, Agre P, Knepper MA (2002) Aquaporins in the kidney: from molecules to medicine. Physiol Rev 82:205–244
36. Portincasa P, Moschetta A, Mazzone A, Palasciano G, Svelto M, Calamita G (2003) Water handling and aquaporins in bile formation: recent advances and research trends. J Hepatol 39:864–874
37. Preston GM, Carroll TP, Guggino WB, Agre P (1992) Appearance of water channels in *Xenopus* oocytes expressing red cell CHIP28 protein. Science 256:385–389
38. Sasaki S, Ishibashi K, Marumo F (1998) Aquaporin-2 and -3: representatives of two subgroups of the aquaporin family colocalized in the kidney collecting duct. Annu Rev Physiol 60:199–220
39. Sasaki S, Ishibashi K, Nagai T, Marumo F (1992) Regulation mechanisms of intracellular pH of *Xenopus laevis* oocyte. Biochim Biophys Acta 1137:45–51
40. Tsukaguchi H, Shayakul C, Berfer UV, Mackenzie B, Devidas S, Guggino WB, VanHoek AN, Hediger MA (1998) Molecular characterization of a broad selectivity neutral solute channel. J Biol Biochem 273:24737–24743
41. Tsukaguchi H, Weremowicz S, Morton CC, Hediger MA (1999) Functional and molecular characterization of the human neutral solute channel aquaporin-9. Am J Physiol 277:F685–F696
42. Vaughan-Jones RD, Peercy BE, Keener JP, Spitzer KW (2002) Intrinsic H^+ ion mobility in the rabbit ventricular myocyte. J Physiol (Lond) 541:139–158
43. Verkman AS, Yang B, Song Y, Manley GT, Ma T (2000) Role of water channels in fluid transport studied by phenotype analysis of aquaporin knockout mice. Exp Physiol 85S:233S–241S
44. Zampighi GA, Kreman M, Boorer KJ, Loo DDF, Bezanilla F, Chandy G, Hall JE, Wright EM (1995) A method for determining the unitary functional capacity of cloned channels and transporters expressed in *Xenopus laevis* oocytes. J Membr Biol 148:65–78
45. Zeuthen T (1980) How to make and use double-barreled ion-selective microelectrodes. Curr Top Membr Trans 13:31–47
46. Zeuthen T, Hamann S, la Cour M (1996) Cotransport of H^+, lactate and H_2O by membrane proteins in retinal pigment epithelium of bullfrog. J Physiol (Lond) 497:3–17
47. Zeuthen T, Klaerke DA (1999) Transport of water and glycerol in aquaporin 3 is gated by H^+. J Biol Chem 274:21631–21636
48. Zeuthen T, Meinild A-K, Klaerke DA, Loo DDF, Wright EM, Belhage B, Litman T (1997) Water transport by the Na^+ / glucose cotransporter under isotonic conditions. Biol Cell 89:307–312
49. Zeuthen T, Zeuthen E, Klaerke DA (2002) Mobility of ions, sugar, and water in the cytoplasm of *Xenopus* oocytes expressing Na^+-coupled sugar transporters (SGLT1). J Physiol (Lond) 542:71–87